



### **Science Arts & Métiers (SAM)**

is an open access repository that collects the work of Arts et Métiers Institute of Technology researchers and makes it freely available over the web where possible.

This is an author-deposited version published in: <https://sam.ensam.eu>  
Handle ID: <http://hdl.handle.net/10985/8198>

#### **To cite this version :**

Anne-Marie RIQUET, Jennifer DELATTRE, Olivier VITRAC, Alain GUINAULT - Design of modied plastic surfaces for antimicrobial applications: Impact of ionizing radiation on the physical and mechanical properties of polypropylene - Radiation Physics and Chemistry - Vol. 91, p.170-179 - 2013

# Design of modified plastic surfaces for antimicrobial applications: Impact of ionizing radiation on the physical and mechanical properties of polypropylene

Anne-Marie Riquet<sup>a,b,c,\*</sup>, Jennifer Delattre<sup>a,b,c</sup>, Olivier Vitrac<sup>a,b,c</sup>, Alain Guinault<sup>d,e</sup>

<sup>a</sup> AgroParisTech, UMR1145 Ingénierie Procédés Aliments, 91300-Massy, France

<sup>b</sup> INRA, UMR1145 Ingénierie Procédés Aliments, 91300-Massy, France

<sup>c</sup> CNAM, UMR1145 Ingénierie Procédés Aliments, 75010- Paris, France

<sup>d</sup> P-2AM, CNAM, 292 rue Saint Martin, 75141 Paris Cedex 03, France

<sup>e</sup> PIMM, Arts et Métiers ParisTech, 151, Bd de l'Hôpital, 75013 Paris, France

## A B S T R A C T

Surface modification of polypropylene (PP) sheets was carried out by radiation induced graft polymerization of hydrophilic functional molecules such as N,N-dimethylacrylamide (DMA) and [2-methacryloyloxy)ethyl] trimethylammonium chloride, which is a quaternary ammonium salt (QAS).

Polypropylene sheets were activated prior to the grafting reaction by using electron beam radiation. The changes in morphology, crystallinity and tensile parameters like deformation and stress at yield and deformation at break of PP after irradiation were investigated. The results showed that a minor crystalline reorganization takes place during the irradiation of PP at 100 kGy.

The grafting has been observed to be strongly dependent on the monomer dilution in the reaction medium. After grafting of QAS (40%) and DMA (20%) it was possible to develop highly hydrophilic surfaces (water contact angle comprised between 30 and 41°). The surfaces of virgin, irradiated and grafted PP were studied using polarized optical microscopy (POM) and scanning electron microscopy (SEM). Spherical particles (i.e. polystyrene or silica beads) adhering to the modified samples were studied according to the surface parameters. Adhesion tests confirmed the strong influence of substrate type (mainly hydrophilicity and roughness) and to a lesser extent underlined the role of electrostatic interactions for the design of plastic surfaces for antimicrobial applications.

## Keywords:

Polypropylene

Physical properties

Surface properties

Electron beam irradiation

Adhesion of particles

## 1. Introduction

Bio-contamination in industry can cause an increase in production costs (reduction in equipment performance, increase in the concentrations of washing chemicals, etc.) and losses associated with the premature degradation of finished products, without

forgetting the costs related to recall procedures for products containing pathogenic micro-organisms and the consequences of toxic infections evoked previously. It is therefore necessary to develop strategies to ensure that surfaces in contact with food-stuffs do not become vehicles for the transmission of pathogenic micro-organisms.

In the agro-food industry, the control of surface bio-contamination through the development of "antimicrobial" materials has only recently been introduced. The development of polymers for food packaging has created enormous interest with respect to the inherent quality of food during long term storage. One of the

\* Corresponding author at: AgroParisTech, UMR1145 Ingénierie Procédés Aliments, 91300-Massy, France. Tel.: +33 169 935119.

E-mail address: anne-marie.riquet@agroparistech.fr (A.-M. Riquet).

requirements of the food packaging has been to utilize antimicrobial packaging so that microbial infection could be controlled in the food items during storage. This is where a substantial amount of work is being directed to the incorporation of antimicrobial agents into such polymers/polymeric devices, so that they acquire ability to kill as well as inhibit the growth and metabolism of microbes.

The incorporation of antimicrobial agents on the surface of packaging materials has been proposed as an appropriate alternative (Rooney, 1995; Vermeiren and Devlieghere, 2002). This can be achieved by blending the antimicrobial agent into the polymer, or by immobilization of the agent on the polymer surface. However, the modification of polymers needs to be carried out in such a way that they acquire polar or ionic functional groups where a specific drug may be linked up. Polypropylene is paraffinic in nature and is devoid of any polar site where the antimicrobial agent may be immobilized. Therefore, the functionalization of the polymer needs to be carried out prior to any antimicrobial treatment. The conception of polymeric materials by radiation induced graft polymerization of chemical substances with specific properties, is interesting because the resultant material not only retains most of its original characteristics but also acquires additional properties of the grafted moiety (Marmey et al., 2003; Bhattacharya and Misra, 2004; Anjum et al., 2008). Another advantage of the process is that the grafting may be accomplished in any form irrespective of the polymer shape and size. However, the structure of the polymer may undergo considerable changes during the graft modification process depending on the nature and the amount of monomer being grafted. These changes may be in terms of the crystallinity, mechanical behavior and thermal stability depending on the compatibility of the grafted component with the backbone matrix (Krupa and Luyt, 2001). The grafted material may behave as the bicomponent system as observed in FEP-g-polystyrene system (Gupta and Scherer, 1993) or else, it may undergo multi-step degradation pattern as evident from the TGA (thermogravimetric analysis) pattern of polyethylene-g-polyacrylamide films (Gupta and Anjum, 2001). The surface confinement of the grafts leaves behind a large fraction of the polymer bulk intact so that mechanical properties of the modified PP are expected to be significantly retained. In spite of the low graft levels, it is bound to show significant impact on the structure and properties of the modified matrix.

The first part of this investigation was aimed at the evaluation of the structural changes in PP matrix occurring during radiation induced graft polymerization of hydrophilic monomers. These changes occurring in terms of mechanical strength, crystalline structure, roughness and wettability are presented in this paper. The second part of this work focused on understanding the mechanisms involved in adhesion phenomena. Particles adhering to the modified samples were studied according to the surface parameters.

## 2. Experimental

### 2.1. Materials

Two types of PP sheets with differing initial surface roughness were studied. The first was a PP named PP micrometer (PP<sub>M</sub>) which is in common commercial grade (PPH7060, Total), shaped by injection molding onto dumbbell specimens (ISO 527 type 5) with the following parameters: melt temperature 220 °C and mold temperature 30 °C. The desired degree of roughness was obtained by preparing the surface of the mold. The second PP had a smoother surface and was referred to PP nanometer (PP<sub>N</sub>) and was supplied in sheet form by Exxon Mobil. These samples,

respectively 1 and 2 mm thick, were used as the substrates during surface modification procedures.

The grafting of hydrophilic monomers onto electron beam irradiated polypropylene was carried out using preirradiation method.

### 2.2. Ionizing radiation treatment

The PP sheets were activated by electron beam irradiation (low energy electron accelerator LAB-UNIT, Energy Science). The energy of the electron beam was 165 keV, with a beam current of 5 mA and a speed of 18 feet min<sup>-1</sup>. Irradiation was performed in air at a dose of 100 kGy.

### 2.3. Grafting reaction

The grafting reaction was performed in a closed reactor (Anjum et al., 2006). The monomer solution was diluted in distilled water (10 and 40%). Mohr's salt was added (0.25%) to prevent the homopolymerization of the monomer solution. The reactor was placed in an oven under argon bubbling to obtain an inert atmosphere. The monomer solution was heated to 60 °C. The irradiated PP sample was then immersed in the solution in the reactor. After the desired period, the grafted PP sample was removed and placed in distilled water in an ultrasonic bath at 40 °C for 10 min to remove all residual traces of the monomer. The grafted PP sample was then dried overnight in an oven at 40 °C.

The PP surface was modified by the grafting of hydrophilic functional molecules such as N,N-dimethylacrylamide (DMA) and [2-(Methacryloyloxy)ethyl]-trimethylammonium chloride, which is a chloride ammonium salt (QAS).

### 2.4. Effects of radiation on polypropylene

#### 2.4.1. Mechanical tests

The tensile tests of PP<sub>M</sub> were carried out using an Instron universal testing machine (model 4507) at room temperature. The tests were performed at 25 mm/min. Tensile stress and deformation at yield and at break were measured. All measurements were done in five replicates and the values averaged.

#### 2.4.2. Observations by optical microscopy

PP<sub>M</sub> crystalline morphology was observed with the help of an optical transmission microscope with polarized light (Nacht, France). Samples of 10 µm thick were prepared by using a microtome (Leica RM 2255, France).

#### 2.4.3. Differential scanning calorimetry (DSC)

DSC studies on samples were carried out using a TA instrument DSC Q100. Around 10 mg samples were loaded into the DSC and a complete cycle was performed comprising a first heating between -10 and 220 °C at 10 °C/min, a cooling to -10 °C at 10 °C/min and a second heating to 220 °C at 10 °C/min. under a nitrogen atmosphere. The heat of fusion ( $\Delta H_f$ ) was calculated from the area under the melting peak. The crystallinity of PP was obtained from the following expression:

$$\text{Crystallinity(\%)} = \frac{\Delta H_f}{\Delta H_f(\text{crys})} \times 100 \quad (1)$$

where,  $\Delta H_f$  is the heat of fusion of the sample and  $\Delta H_f(\text{crys})$  is the heat of fusion of 100% crystalline

For PP  $\Delta H_f(\text{crys})$  was taken as 209 J/g (Mark et al., 1986).

#### 2.4.4. X-ray diffraction

The crystalline structure of the film samples was investigated by wide-angle X-ray scattering (WAXS) by means of a X'Pert (Panalytical) diffractometer (Cu-K $\alpha$  radiation). The high voltage was fixed at 40 kV and the tube current was set at 40 mA.

#### 2.5. Characterization of surface properties

##### 2.5.1. Contact angle measurement

Contact angle measurements can determine the hydrophilic/hydrophobic nature of surfaces under study, as well as their energy characteristics.

Contact angles were measured with a G40 Goniometer (Krüss, France) at room temperature using the sessile drop method with high purity water (Millipore milliQ).

##### 2.5.2. Roughness

Surface roughness was determined using a method of non-contact with the analyzed surface (Altisurf<sup>®</sup> 500, Altimet). A probe equipped with a high chromatic aberration lens breaks a light beam with lengths of monochromatic waves over a distance of 300  $\mu$ m. Depending on the topography of the surface analyzed, certain wavelengths will be reflected. In this case, they were interpreted in terms of altitude and were able to determine parameter Ra (arithmetic roughness deviations from the mean), expressed in micrometers.

##### 2.5.3. Adhesion of particles

The adhesion of particles on PP surfaces enables a count of the number of adhered particles and comparison of the results as a function of surface parameters.

The adhesion of 2  $\mu$ m-diameter silica beads (Bangs Laboratories) and PS beads (Sigma) was studied. The PP sheets were immersed in a solution of beads at  $5 \times 10^{-3}\%$  in an NaCl solution at  $1.5 \times 10^{-3}$  M. For the adhesion of silica and PS beads, samples are immersed for 1 and 3 h, respectively. This period was determined from the sedimentation time of each type of beads. After the adhesion test, the samples were rinsed gently with ultra-pure water to remove non-adherent beads and then dried overnight in an oven at 40 °C.

The surfaces were examined under an optical microscope (BX51, Olympus) through a 40x objective. The microscope was connected to a camera (SC30, Olympus) and a computer for image acquisition and storage.

Ten photos were taken of each sample at different locations. For the rougher surfaces, several photos were taken at each location by varying the depth of field.

Images were analyzed to determine the number of adherent beads using a image analysis software (Image Tool).

##### 2.5.4. Auto-correlation analysis

The texture of images containing fluorescent particles was characterized in terms of self-similarity by translation via 2D normalized image autocorrelations. By noting  $f(i,j) = (I - \langle I \rangle) / sd(I)$  as the normalized brightness of an  $N_1 \times N_2$  fluorescence image  $I(i,j)$ , where  $\langle I \rangle$  and  $sd(I)$  are the average and the standard deviation of  $I$  respectively, its auto-correlation was calculated for both positive and negative lags ( $k = -N_1, N_1, l = -N_2, N_2$ ) as:

$$R_{II}(k, l) = \frac{1}{(2N_1 + 1)(2N_2 + 1)} \sum_{i=-N_1}^{N_1} \sum_{j=-N_2}^{N_2} f(i, j) f(i+k, j+l) \quad (2)$$

$R_{II}(k, l)$  was calculated efficiently for  $N_1$  and  $N_2$  chosen as powers of two so that fast 2D discrete Fourier transforms could be used. Indeed, the Fourier transform of  $R_{II}$  is also defined as the product of the Fourier transform of  $I$  and of its complex conjugate.

$R_{II}$  supplied a significant number of informative details on the spatial distribution of particles and on the mode of adhesion, in particular regarding possible correlations with the type and orientation of defects on the surface. The span and direction of the decrease in  $R_{II}$  indicated the size of possible groups of particles (i.e. agglomerates) and their preferential orientations. Spatial isotropy was detected from the circular symmetry of  $R_{II}$ . The periodicity of the peaks of  $R_{II}$  assessed the spatial periodicity of sites where the particles accumulated. Finally, the reduction in the envelope gave an idea of the self-similarity between accumulation sites on a large scale.

### 3. Results and discussion

#### 3.1. Effects of irradiation on polypropylene

##### 3.1.1. Mechanical properties

Mechanical properties were measured on PP<sub>M</sub> before and after irradiation. Table 1 shows that the stress and deformation at yield were not affected by irradiation, while deformation at break markedly decreased. The irradiation of injected PP sheets led to a brittle material, with a maximum elongation at break of around 10%, while the elongation at break of the virgin PP<sub>M</sub> was around 156%. These values, and particularly that of the virgin PP<sub>M</sub>, were low when compared with values found in the literature (Lu and Guan, 2000). This result might have been related to residual stresses in the material caused by the low mold temperature and the low melt temperature of injection, considering the relatively low thickness of the sample (1 mm). A sharp decrease of elongation at break after e-beam treatment was consistent with findings in the literature (Phillips and Burnay, 1991; Lu and Guan, 2000; Pawde and Parab, 2011). This could be attributed to a radiation induced chain scission process in the PP matrix.

##### 3.1.2. Differential scanning calorimetry (DSC)

During our experiments we investigated both the first and the second heating scan. This is particularly important for polyolefins cross-linked with irradiation, where significant differences between the first and the second scan were observed. There was, however, no significant change in the thermograms of virgin PP<sub>M</sub> after the first and second heatings (Table 2). The second scan of Virgin PP<sub>M</sub> (which basically is a measurement of the re-melting of the sample and so the image of the polymer without its processing) shows a single melting peak (160 °C), suggesting that PP is characterized by one crystalline form (Yagoubi et al., 1999). The exposure of PP<sub>M</sub> to a dose of 100 kGy by electron beam caused some changes in the thermograms, especially in the second heating (Fig. 1). The melting peak became broader and the origin of another peak displaced toward a lower temperature was observed (153 °C). Similar behavior has been reported by several authors (Minkova et al., 1988; Kokostoski et al., 1990; Riquet et al., 2011). Changes to the peak for the irradiated PP sample may have been due to crystalline reorganization during irradiation with 100 kGy. The dual mode of the melting peaks could have been attributed to structural changes. Multiple endotherms are observed in a wide variety of semicrystalline polymers. This situation

**Table 1**

Mechanical properties of PP<sub>M</sub> before and after irradiation in air at a dose of 100 kGy.

	Yield stress (MPa)	Yield deformation (%)	Deformation at break (%)
Virgin PP <sub>M</sub>	36.2 $\pm$ 0.50	5.97 $\pm$ 0.18	156 $\pm$ 7.0
Irradiated PP <sub>M</sub>	35.2 $\pm$ 0.26	5.18 $\pm$ 0.16	10 $\pm$ 1.0



**Table 2**

Values of heat of fusion, melting temperature and crystallinity of virgin and irradiated PP<sub>M</sub> after the first and the second scan.

Sample	Melting Temperature T <sub>m</sub> (°C)		Heat of Fusion ΔH <sub>f</sub> (J/g)		Crystallinity (%)	
	First scan	Second scan	First scan	Second scan	First scan	Second scan
Virgin PP <sub>M</sub>	162.7 ± 1.0	160.7 ± 2.0	96.8 ± 1.5	101.2 ± 1.3	46.3 ± 0.7	48.4 ± 0.6
Irradiated PP <sub>M</sub>	159.9 ± 1.3	153.4 ± 0.8 160.3 ± 1.0	90.9 ± 2.2	75.0 ± 0.9 25.8 ± 0.7 (100.8)	43.5 ± 1.0	48.2 ± 0.3

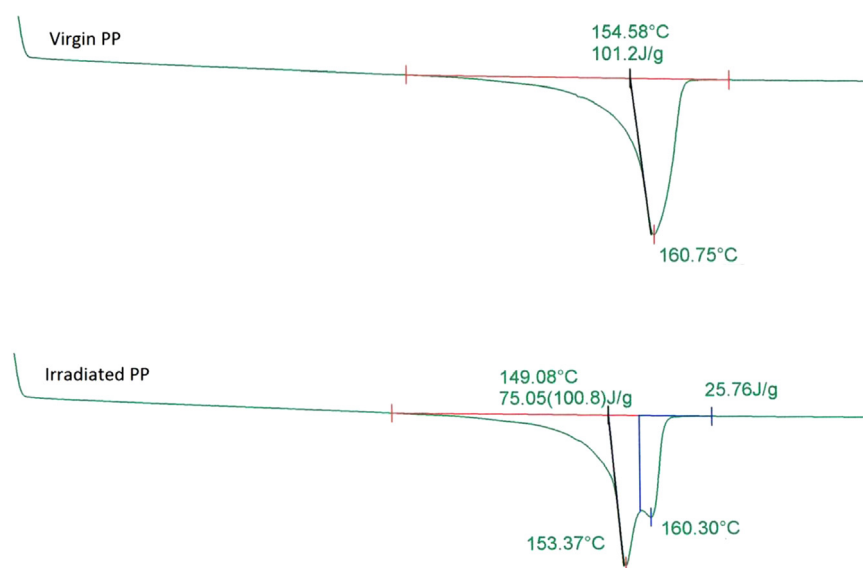


**Fig. 1.** DSC thermograms of virgin and irradiated polypropylene micrometer PP<sub>M</sub> (Second Heating).

may arise from segregation effects linked to molecular weight, among other parameters (Perera et al., 2004).

### 3.1.3. XRD

The different X-ray diffraction patterns of virgin and irradiated PP samples are presented in Fig. 2. The crystalline reflections of α phase for virgin and irradiated PP<sub>M</sub> occurred at identical angles. The hexagonal β phase was identified by a high maximum for the (300)β plane. The relative amount of the β phase (K value) was determined by the ratio between the intensity I<sub>β</sub> of the peak for the (300) diffracting plane and the sum of the intensities I<sub>α1</sub>, I<sub>α2</sub> and I<sub>α3</sub> of the (110), (040) and (130) planes as well as I<sub>β</sub> of the (300) peak. Mathematically, the K value was given by Shi and Zhang (1982):

$$K = \frac{1\beta}{I\alpha1 + I\alpha2 + I\alpha3 + 1\beta} \quad (3)$$

Interestingly, the exposure of PP to electron beam caused a slight enhancement in the relative content of the β form, from 8.6% to 12.7% (Mishraa et al., 2001). This could be attributed to the fact that chain scission dominates during electron beam irradiation and these short chains tend to reorganize themselves subsequently into crystalline structures (Sen and Kumar, 1995). These results reinforced the DSC observations that a crystalline reorganization occurred during the irradiation of PP.

Optical microscopy observations under polarized light showed that treatment with ionizing radiation (β, 100 kGy) significantly altered the size of the spherulites (Fig. 3). Relatively small at the surface of the control material, they were seen to be considerably larger in the irradiated samples. These changes may have been responsible for impairing the mechanical properties of the modified materials.

Because of the energy of the electron beam (165 keV), the depth of electron penetration into the matrix was about 300 μm.

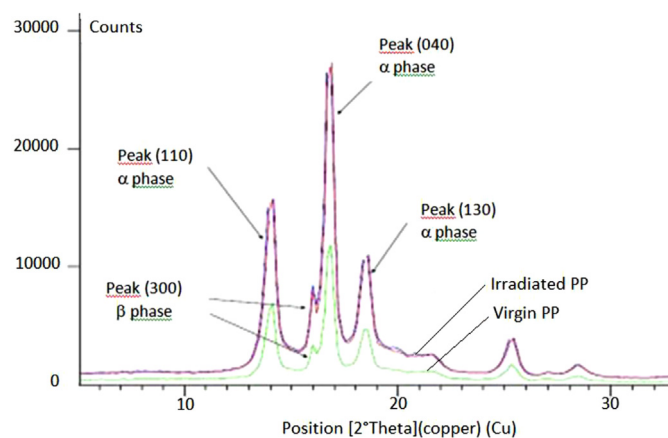


**Fig. 2.** X-ray diffraction of the β-form from virgin and irradiated polypropylene micrometer PP<sub>M</sub>.

For this reason, 100 kGy caused particular alterations to the irradiated surface of the film.

The results presented in the second section of this paper concern those obtained after the surface modification of micrometric PP (PP<sub>M</sub>). Because of this, we have identified the most relevant modifications for further study, and modified the surfaces of nanometric PP (PP<sub>N</sub>) at the selected proportions of monomers.

### 3.2. Radiation induced graft polymerization reaction

The curves shown in Fig. 4 reflect variations in the degree of grafting for N,N-dimethylacrylamide (DMA) as a function of time and at different monomer concentrations. In the case of pure DMA and diluted monomers (10–80%), the degree of grafting increased

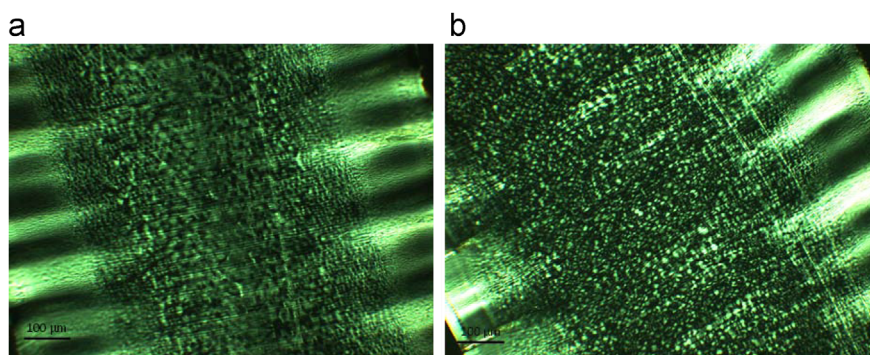


**Fig. 3.** Observation by optical microscopy in polarized light of (a) virgin and (b) irradiated ( $\beta$ , 100 kGy) polypropylene micrometer ( $PP_M$ ).

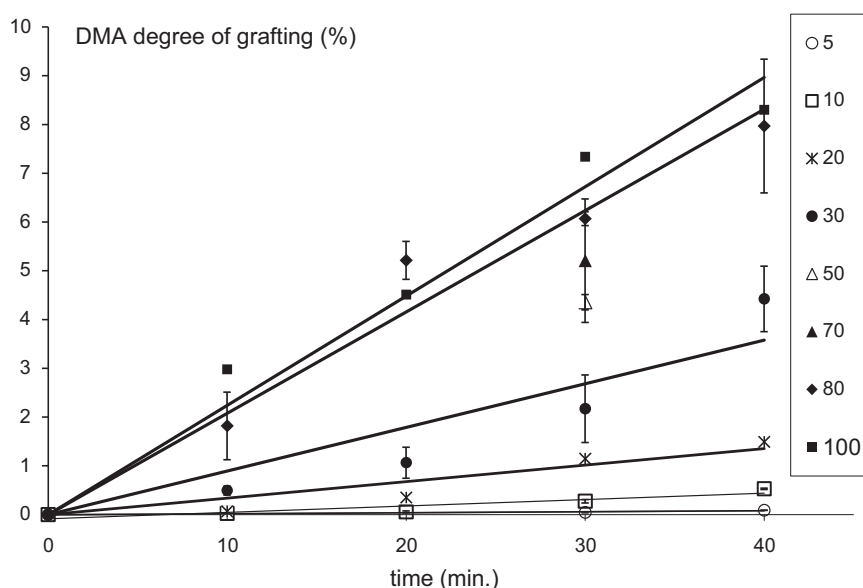


**Fig. 4.** Variation of the degree of grafting for N,N-dimethylacrylamide (DMA) with the reaction time at different monomer concentrations (%). Preirradiation dose 100 kGy; temperature 60 °C.

over time, and even after 40 min was proportional to the percentage of monomers present in the reaction medium.

The degree of grafting with QAS diluted at 40% was at the limit of the threshold of detection by weighing ( $10^{-4}$  g). This was probably due to the viscosity of this compound, its steric hindrance and the surface properties of PP, an apolar and hydrophobic material.

### 3.2.1. Characterization of surface properties

To analyze surface wettability, contact angle measurements were performed on unmodified (virgin and irradiated  $PP_M$ ) and previously modified (grafted)  $PP_M$  surfaces and the results are presented in Table 3. The water contact angle is the most convenient parameter to analyze the surface hydrophilic/hydrophobic properties of modified polymeric surfaces.

The contact angles of virgin and irradiated  $PP_M$  were  $94 \pm 3^\circ$  and  $83 \pm 4^\circ$ , respectively. However, all the grafted  $PP_M$  displayed a downward trend, with an increase in the degree of grafting.

In line with the results obtained by Chen et al. (2006) grafting with DMA resulted in a marked increase in hydrophilicity, whatever the DMA percentage in the reaction medium ( $30 \leq \theta \leq 41^\circ$ ).

After the grafting of QAS, we obtained highly hydrophilic surfaces ( $\theta = 20^\circ$ ).

The results shown in Table 4 and Fig. 5 underline the influence of the degree of grafting on surface topography. At extremely low degree of grafting (at the limit of the threshold of detection by weighing) the roughness of micrometric PP ( $PP_M$ ) or nanometric PP ( $PP_N$ ) was not modified (0.25 and 0.04  $\mu\text{m}$ , respectively). On the other hand, as from 0.1% of grafting, the roughness of  $PP_N$  increased significantly (from 0.04 to 0.08  $\mu\text{m}$ ) while that of  $PP_M$  (0.25  $\mu\text{m}$ ) remained unchanged for as long as the degree of grafting remained lower than 0.2%. For degree of grafting higher than 0.2% there was a linear relationship between the degree of grafting and the roughness of the surface (Fig. 6).

The increase in roughness related to grafting was more significant on nanometric substrates than on micrometric substrates, whatever the degree of grafting.

A scanning electron microscope (SEM) was used to visualize the morphologies of PP samples before and after grafting (Fig. 7). It could be seen that the surface of virgin  $PP_M$  displayed some parallel strips not observed on  $PP_N$ , which looked smooth (Fig. 7 a, b). This result, already reported in the literature, most probably resulted from the shape of the PP sheets produced by injection. Ionizing radiation treatment (100 kGy) did not seem to affect the surface topography of native material whether it was micrometric or nanometric (Fig. 7 c, d). On the other hand, it was interesting to note that the grafting of hydrophilic monomers rigorously followed the surface topography of the substrate concerned and

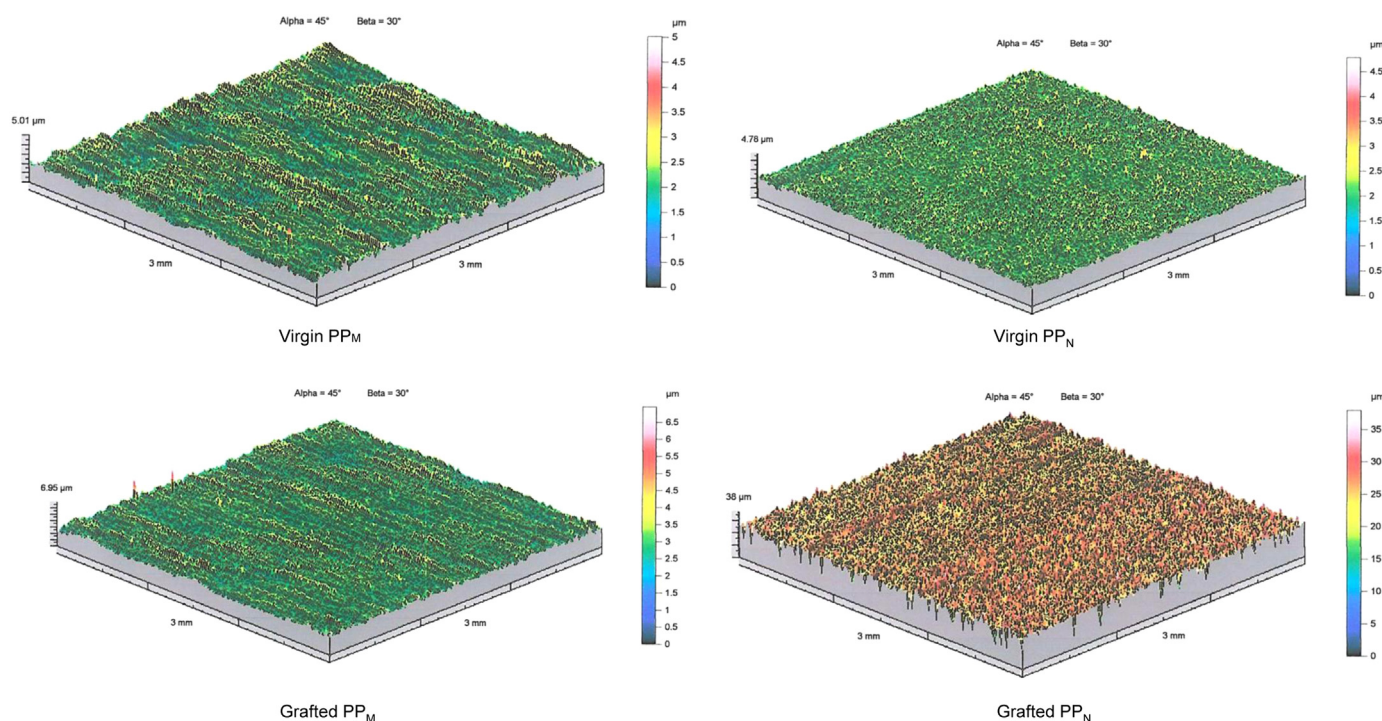
**Table 3**Water contact angles for virgin PP<sub>M</sub>, irradiated PP<sub>M</sub>, and PP<sub>M</sub> grafted with DMA or QAS.

Monomer	Monomer concentration (%)	Degree of grafting (%)	Contact angle (deg.)
Virgin PP <sub>M</sub>	–	–	94 ± 3
Irradiated PP <sub>M</sub>	–	–	83 ± 4
PP <sub>M</sub> -DMA	10	0.1	41 ± 5
	20	1.5	34 ± 6
	30	2.1	32 ± 4
	40	4.3	30 ± 4
	100	8.5	29 ± 2
PP <sub>M</sub> -SAQ	40	~0	20 ± 4

**Table 4**

Variations in surface topography according to the degree of grafting.

Micrometric PP <sub>M</sub>		Nanometric PP <sub>N</sub>	
Degree of grafting (%)	Roughness (μm)	Degree of grafting (%)	Roughness (μm)
c~ 0	0.25	~0	0.04
0.02	0.25	0.01	0.05
0.21	0.26	0.04	0.04
0.82	0.49	0.09	0.08
1.27	0.65	3.24	3.02
4.32	1.74		

**Fig. 5.** Surface topographies of virgin micrometric or nanometric polypropylene (PP<sub>M</sub>, PP<sub>N</sub>) and PP<sub>M</sub> or PP<sub>N</sub> grafted with respectively 0.8% and 3.2% of N,N-dimethylacrylamide (DMA).

resulted in a very different surface structure, depending on whether a PP<sub>M</sub> or a PP<sub>N</sub> was considered.

A marked increase in the relief of the parallel strips was observed after grafting on a micrometric substrate. This phenomenon was especially significant when the degree of grafting was high (Fig. 7e, g). In the case of PP<sub>N</sub>, at grafting percentages of about 0.1% the surface of the material displayed a relief with an “orange

peel” structure (Fig. 7 f). A high degree of grafting (3%) tended to affect this structure (Fig. 7h).

### 3.2.2. Adhesion of particles

Prior to bacterial adhesion, tests of particle adhesion (2 μm diameter polystyrene or silica beads) were performed on native

and modified PP surfaces in order to clarify the mechanisms involved in adhesion phenomena. Indeed, these beads constitute a less complex model to understand adhesion phenomena insofar as their surface properties do not vary during contact with a surface, unlike micro-organisms.

The contact angle method, coupled with the Young-van Oss equation made it possible to determine the energy characteristics of the silica and PS beads used during adhesion tests (Table 5). It can be noted that, as expected, the commercial PS beads were more hydrophobic than the silica beads. PS beads also displayed a slightly lower polar character (3.8 instead of 6.3 mJ/m<sup>2</sup>) and a similar capacity for the exchange of Lifshitz-van der Waals interactions ( $\gamma_{LW}$  40 mJ/m<sup>2</sup>). The zeta potential of PS beads at the pH of the NaCl solution at  $1.5 \times 10^{-3}$  M was -25 mV.

For the adhesion tests, PP samples were immersed in a solution of beads at  $5 \times 10^{-3}\%$  diluted in an NaCl solution at  $1.5 \times 10^{-3}$  M for 1 h (silica beads) and 3 h (PS beads).

As during the grafting stages, optical microscope observations appeared to indicate that the adhesion of PS particles was governed by surface topography. On PP<sub>M</sub>, the beads aligned themselves along the ridges, while they did not adopt any preferential orientation on PP<sub>N</sub> (Fig. 8). In order to confirm or refute these observations, an auto-correlation analysis was performed. This mathematical tool enables a comparison of the

relative positioning of particles and the tracing of curves that correspond to their preferred alignments. The results presented in Fig. 9a,c confirmed the preferred linear orientation of PS beads on the surface of native micrometric PP (Fig. 9 a) or on PP<sub>M</sub> modified by grafting with 40% DMA, i.e. a surface with more marked roughness (Ra 1.74  $\mu$ m) (Fig. 9 c). By contrast, on nanometric substrates, bead adhesion did not follow any preferential direction, whatever the degree of roughness (Fig. 9 b, d). A similar behavior was observed with the silica beads (Fig. 10). However, under monitored acquisition conditions, the adhesion mode of the beads did not appear to influence the number of beads adhering to the substrate.

If surface roughness was considered, it could be seen that the percentage coverage of PP by PS beads was always greater when the surface was rough. By contrast, regarding their hydrophilic/hydrophobic character, PS beads displayed much greater affinity for hydrophobic control substrates ( $\theta=95^\circ$ ) than for highly hydrophilic modified substrates ( $\theta=40^\circ, 30^\circ$  or  $20^\circ$ ) whatever the degree of surface roughness (Fig. 11).

Using silica beads, the percentage coverage of hydrophilic substrates was significantly higher (factor ~15) than that seen on control substrates. Crossing of these results suggested that the wettability of the surface had a predominant effect on particle adhesion, while topography (roughness) exerted only a secondary effect.

With respect to short and long distance interactions, PP modified with DMA displayed characteristics similar to those of polystyrene beads. Thus no attractive or repulsive interactions could be generated. By contrast, electrostatic interactions were

**Table 5**

Energy characteristics of silica and polystyrene beads used in adhesion tests.

	Silica beads	Polystyrene beads
$\theta$ water (deg.)	$63 \pm 8$	$108 \pm 2$
$\theta$ formamide (deg.)	$51 \pm 7$	$93 \pm 5$
$\theta$ diiodomethane (deg.)	$51 \pm 5$	$54 \pm 3$
$\gamma_{LW}$ (mJ/m <sup>2</sup> )	33.6	31.9
$\gamma_{AB}$ (mJ/m <sup>2</sup> )	6.1	3.8
$\gamma_T$ (mJ/m <sup>2</sup> )	39.7	35.7

With  $\gamma_T$  energy of surface,  $\gamma_{AB}$  and  $\gamma_{LW}$  the polar and Lifshitz-van der Waals components of surface tension respectively;  $\theta$  are the contact angles in pure liquids of water, formamide and diiodomethane.

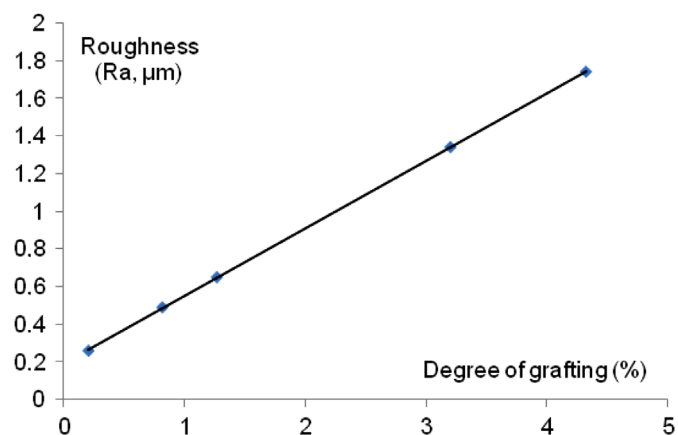


**Fig. 6.** Variation of the roughness of polypropylene micrometer PP<sub>M</sub> with the degree of grafting.

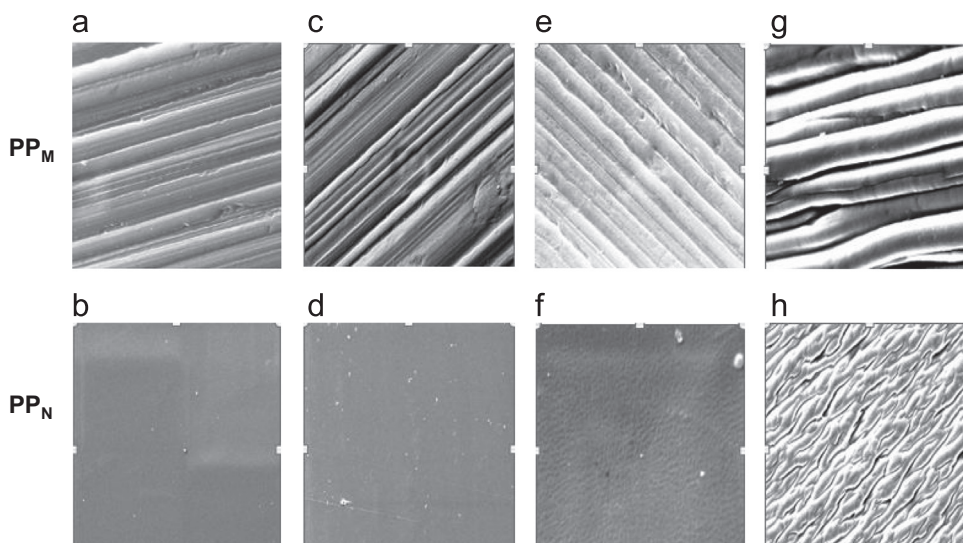


**Fig. 7.** Scanning Electron Microscopy images of polypropylene micrometer PP<sub>M</sub> (on the top) and polypropylene nanometer PP<sub>N</sub> (at the bottom); a, b virgin PP; c, d irradiated PP; e, f grafted PP with diluted DMA (10%); and g, h grafted PP with diluted DMA (40%).



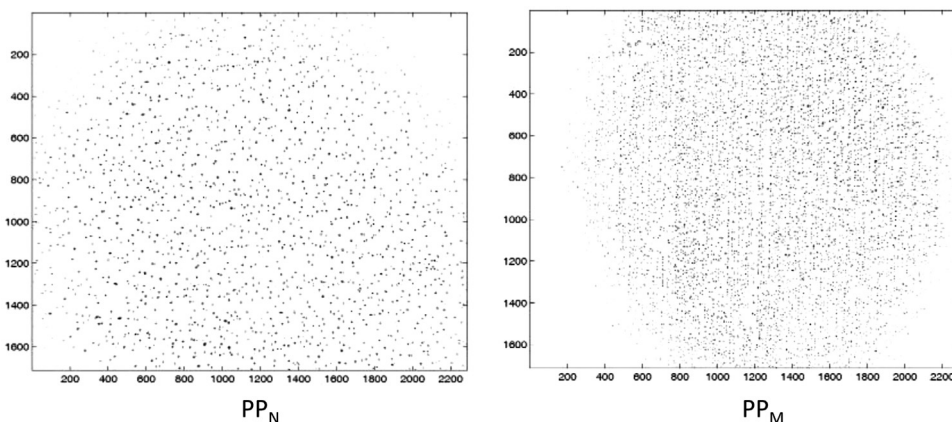


**Fig. 8.** Images of adherent PS beads observed under an optic microscope (BX51, Olympus) through a 40x objective for polypropylene micrometer  $PP_M$  (b) and polypropylene nanometer  $PP_N$  (a).

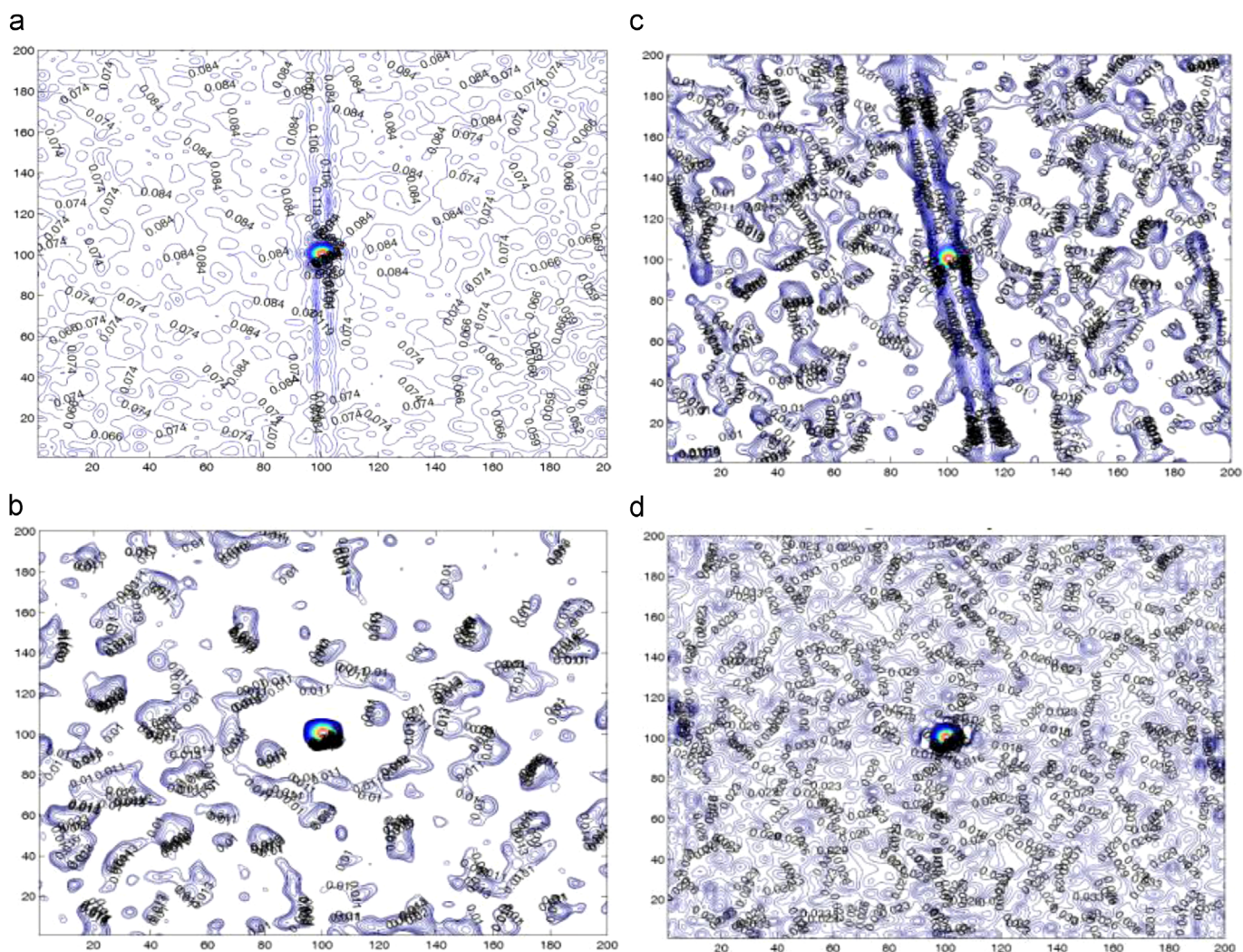


**Fig. 9.** Images of auto-correlation analysis of PS beads on virgin  $PP_M$  (a), virgin  $PP_N$  (b), grafted  $PP_M$  with 40% diluted DMA (c) and grafted  $PP_N$  with 40% diluted DMA (d).

attractive between QAS-modified surfaces ( $\zeta=102$  mV) and polystyrene beads ( $\zeta=-25$  mV), thus favouring the approach of beads to the surface of PP. In principle, the influence of Lewis acid-base interactions is much greater than that of electrostatic interactions. However, these are short distance interactions, and it is necessary for the bead and the substrate to be relatively close for these forces

to become effective. These conditions were probably not achieved between the polystyrene beads and QAS-modified surfaces (Fig. 11). The initial adhesion tests performed by sedimentation for 24 h at 20 °C with *Listeria monocytogenes* (LM) demonstrated a difference in the bioadhesive behavior of the strain employed, as a function of the physicochemical properties of the substrate surface tested.



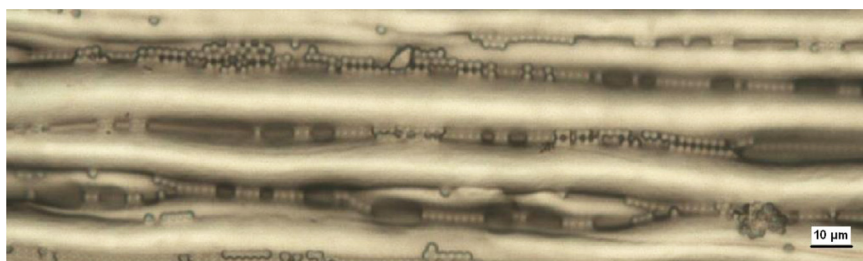


**Fig. 10.** Images of adherent silica beads observed under an optic microscope (BX51, Olympus) through a 40x objective for polypropylene micrometer PP<sub>M</sub> grafted with 3.2% of DMA.

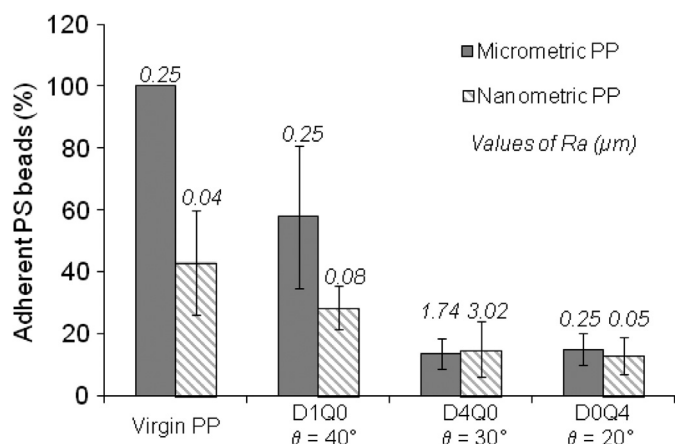


**Fig. 11.** Variation of the percentage adhesion of PS beads with the roughness of unmodified and modified PP surfaces.

On SAQ-grafted PP substrates, microbiological analyses demonstrated an increase of around  $2 \log_{10}$  CFU/cm<sup>2</sup> when compared with the control PP, whatever the degree of surface roughness. These results suggest that the hydrophilicity of the surface was not the only parameter influencing LM adhesion. Attractive interactions between SAQ-grafted materials ( $\zeta = +102$  mV) and LM ( $\zeta = -41$  mV) thus favoured bioadhesion.

#### 4. Conclusion

The aim of these studies was to modify the surface of PP at a low grafting level and to introduce hydrophilicity by using two monomers, a quaternary ammonium salt (QAS) and N,N-dimethylacrylamide (DMA), so that these surfaces could then be analyzed with respect to bacterial adhesion. The results show that electron beam induced preirradiation grafting of monomers onto polypropylene offers an attractive means of modifying polymers for specific applications. In terms of crystalline structure, X-ray diffraction and DSC revealed that the impact of electron beam treatment on structural changes in the PP matrix was not really significant when compared to the virgin PP. However, the deformation at break rendered the material brittle. This may be related to the size of the spherulites that had grown in the irradiated samples. Furthermore, the development of new molding and ionization (lower doses) conditions could maintain the ductility of the PP supports.

The degree of grafting and physicochemical characteristics of polypropylene surfaces functionalized by the radiation induced grafting of hydrophilic monomers were dependent on the operating conditions, such as the concentration in monomers, the duration of exposure or temperature. When these conditions were perfectly controlled, it was possible to develop highly hydrophilic surfaces ( $20^\circ < \theta_{\text{water}} < 35^\circ$ ) with excellent reproducibility.

The grafting of DMA on a PP substrate resulted in a hydrophilic surface whatever the percentage monomer content in the reaction medium and the degree of grafting. These results constitute an unique concept in the grafting process where just a single aspect of the monomer concentration can alter the surface and construct the PP matrix without this involving any significant alteration to the bulk structure.

Grafting led to significant changes to structural morphology, particularly when the initial substrate was smooth. However, under monitored acquisition conditions, the mode of adhesion did not seem to affect the number of particles that had adhered, whatever their nature (silica or PS beads).

Image analysis of the adherent particles revealed that surface hydrophilicity played a major role in particulate adhesion, while topography (roughness) only had a secondary effect. However, electrostatic interactions appeared to predominate within the bioadhesion mechanism.

More studies will now be performed in order to validate these results, using micro-organisms such as *Escherichia Coli*, *Listeria Monocytogenes* or *Pseudomonas Aeruginosa* which are responsible for numerous, more or less severe, outbreaks of food poisoning.

#### References

- Anjum, N., Moreau, O., Riquet, A.M., 2006. Surface designing of polypropylene by critical monitoring of the grafting conditions. *J. Appl. Polym. Sci.* 100, 546–558.
- Anjum, N., Bellon-Fontaine, M.N., Herry, J.M., Riquet, A.M., 2008. A novel process to develop modified polymeric surfaces for the analysis of bacterial adhesion: surface properties and adhesion test. *J. Appl. Polym. Sci.* 109, 1746–1756.
- Bhattacharya, A., Misra, B.N., 2004. Grafting: a versatile means to modify polymers—techniques, factors and applications. *Prog. Polym. Sci.* 29, 767–814.
- Chen, C.P., Ko, B.T., Lin, S.L., Hsu, M.Y., Ting, C., 2006. Hydrophilic polymer supports grafted by poly(ethylene glycol) derivatives via atom transfer radical polymerization. *Polymer (Guildf)* 47, 6630–6635.
- Gupta, B., Anjum, N., 2001. Development of membranes by radiation grafting of acrylamide into polyethylene films: Characterization and thermal investigations. *J. Appl. Polym. Sci.* 82, 2629–2635.
- Gupta, B., Scherer, G.G., 1993. Radiation induced grafting of styrene onto Fepa films - Structure and thermal behavior of copolymers. *Angew. Makromol. Chem.* 210, 151–164.
- Lu, D.P., Guan, R., 2000. Structure and mechanical properties of isotactic polypropylene and iPP/talc blends functionalized by electron beam irradiation. *Polym. Int.* 49, 1389–1394.
- Kokotoski, D., Stojanovic, Z., Kacarevicpopovic, Z., 1990. The effect of antioxidants on the morphology of gamma irradiated isotactic polypropylene. *Radiat. Phys. Chem.* 35, 190–196.
- Krupa, I., Luyt, A.S., 2001. Physical properties of blends of LLDPE and an oxidized paraffin wax. *Polym. Degrad. Stabil.* 72, 505–510.
- Mark, H.F., Bikales, N.M., Overberger, C.G., Menges, G. (Eds.), 1986. *Encyclopedia of Polymer Science and Technology*, 4. Wiley, p. 487.
- Marmey, P., Porte, M.C., Baquay, C., 2003. PVDF multifilament yarns grafted with polystyrene induced by  $\gamma$ -irradiation: influence of the grafting parameters on the mechanical properties. *Nucl. Instrum. Meth. B* 208, 429–433.
- Minkova, L., Lefterova, E., Koleva, T., Nedkov, E., Nikolova, M., 1988. Thermogravimetry and differential scanning calorimetry of gamma irradiated polypropylene films. *Colloid Polym. Sci.* 266–898.
- Mishra, R., Tripathy, S.P., Dwivedi, K.K., Khathing, D.T., Ghosh, M.M., 2001. Electron induced modification in polypropylene. *Radiat. Meas.* 33, 845–850.
- Pawde, S.M., Parab, S., 2011. Effect of electron beam irradiation on mechanical and dielectric properties of polypropylene films. *J. Appl. Polym. Sci.* 119, 1220–1229.

- Perera, P., Albano, C., Gozalez, J., Silva, P., Ichazo, M., 2004. The effect of gamma radiation on the properties of polypropylene blends with styrene-butadiene-styrene copolymers. *Polym. Degrad. Stabil.* 85, 741.
- Phillips, D.C., Burnay, S.G., 1991. Irradiation Effects on Polymers. In: Glegg, D.W., Collyer, A.A. (Eds.), 9. Elsevier Applied Science-London, p. 345.
- Riquet, A.M., Rohman, G., Guinault, A., Demilly, M., 2011. Surface modification of polypropylene by radiation grafting of hydrophilic monomers: physicochemical properties. *Surf. Eng.* 27, 234–241.
- Rooney, M.L. (Ed.), 1995. *Active Food Packaging*. Blackie Academic and Professional, Glasgow.
- Sen, K., Kumar, P., 1995. Influence of gamma irradiation on structural and mechanical properties of polypropylene yarn. *J. Appl. Polym. Sci.* 55, 857–863.
- Shi, G.Y., Zhang, J.Y., 1982. Study on beta form polypropylene. *Kexue Tongbao* 27, 290–294.
- Vermeiren, L., Devlieghere, F., Debevere, J., 2002. Effectiveness of some recent antimicrobial packaging concepts. *Food. Addit. Cont.* 19, 163–171.
- Yagoubi, N., Peron, R., Legendre, B., Grossiord, J.L., Ferrier, D., 1999. Gamma and electron beam radiation induced physico-chemical modifications of poly(propylene). *Nucl. Instrum. Meth. B* 151, 247–254.